IEEE Access
Multidisciplinary | Rapid Review | Open Access Journal

IEEE POWER & ENERGY SOCIETY SECTION

Received March 15, 2021, accepted April 8, 2021, date of publication April 16, 2021, date of current version April 26, 2021.

Digital Object Identifier 10.1109/ACCESS.2021.3073779

Distributed Robust Finite-Time Secondary Control for Stand-Alone Microgrids With Time-Varying Communication Delays

AMEDEO ANDREOTTI, (Senior Member, IEEE), BIANCA CAIAZZO, ALBERTO PETRILLO, AND STEFANIA SANTINI, (Member, IEEE)

Department of Electrical Engineering and Information Technology, University of Naples Federico II, 80125 Naples, Italy

Corresponding author: Bianca Caiazzo (bianca.caiazzo@unina.it)

ABSTRACT In this paper we consider the problem of restoring the voltage for stand-alone inverter-based Microgrids despite the effects of the time-delays arising with the information exchange among the electrical busses. To guarantee that all Distributed Generators (DGs) reach in a finite-time and maintain the voltage set-point, as imposed by a virtual DG acting as a leader, we suggest a novel robust networked-based control protocol that is also able to counteract both the time-varying communication delays and natural fluctuations caused by the primary controllers. The finite-time stability of the whole Microgrid is analytically proven by exploiting Lyapunov-Krasovskii theory and finite-time stability mathematical tools. In so doing, delay-dependent stability conditions are derived as a set of Linear Matrix Inequalities (LMIs), whose solution allows the proper tuning of the control gains such that the control objective is achieved with required transient and steady-state performances. A thorough numerical analysis is carried out on the IEEE 14-bus test system. Simulation results corroborate the analytical derivation and reveal both the effectiveness and the robustness of the suggested controller in ensuring the voltage restoration in finite-time in spite of the effects of time-varying communication delays.

INDEX TERMS Secondary voltage control, islanded microgrid, multi-agent systems, time-varying communication delay, robust control strategy, finite-time stability, Lyapunov-Krasovskii theory, IEEE 14-bus test system.

NOMENCLATURE

δ_i	Phase angle of the i-th DG
ω_i	Frequency of the i-th DG
v_i	Voltage of the i-th DG
k_{Pi}	Frequency droop gain of the i-th DG
k_{Qi}	Voltage droop gain of the i-th DG
k_{vi}	Voltage primary control gain
u_i^{ω}	Frequency secondary control input of the i-th DG
u_i^{V}	Voltage secondary control input of the i-th DG
$\omega^{\star}$	Frequency set-point
$v^{\star}$	Voltage set-point
P_i^m	Real measured power via the i-th fist-order low pass filter
Q_i^m	Reactive measured power via i-th fist-order low pass filter
τ_{Pi}	Time constants of the i-th first order low pass filter associated with real power
τ_{Qi}	Time constants of the i-th first order low pass filter associated with reactive power
P_i	Active power output of the i-th DG
Q_i	Reactive power output of the i-th DG
$\hat{P}_\rho$	Active injected power of the ρ-th electrical bus
$\hat{Q}_\rho$	Reactive injected power of the ρ-th electrical bus
$Y_{\rho k}$	Admittance between the ρ-th and the k-th bus
$G_{\rho k}$	Conductance between the ρ-th and the k-th bus
$B_{\rho k}$	Susceptance between the ρ-th and the k-th bus
P_{L_ρ}	Active power of the ρ-th ZIP load
Q_{L_ρ}	Reactive power of the ρ-th ZIP load
$P_{1\rho}, Q_{1\rho}$	Nominal impedance loads constants
$P_{2\rho}, Q_{2\rho}$	Nominal current loads constants
$P_{3\rho}, Q_{3\rho}$	Nominal power loads constants
Π^{Q}	Threshold for total reactive power output of the i-th DG

The associate editor coordinating the review of this manuscript and approving it for publication was Ning Kang.

Π^P	Threshold for total active power output of the i-th DG
v_ρ	Measured voltage of the ρ-th bus
δ_ρ	Measured phase angle of the ρ-th bus
N	Numbers of DGs within the MG
M	Numbers of local loads within the MG

I. INTRODUCTION

Over the past few years, Microgrids (MGs) have received considerable attention due to their potential role in mitigating consequences of sudden grid interruption, guaranteeing an uninterrupted energy supply for the electrical loads, and reliable grid operation [1]. These medium-voltage/low-voltage (MV/LV) small-scale power networks are typically employed for supporting the electrical network in remote sites and rural areas (e.g. consisting in homes/building networks or industrial plants) [2], thus providing an innovative, economic and environmental-friendly solution [3]. Moreover, MGs may be needed also in areas with critical loads, such as banking systems, semiconductor industries, hospitals and data centers [4]. Heterogeneous Distributed Generators (DGs), Energy Storage Systems (ESSs) and loads are the main entities involving within a MG, which are collectively managed in order to increase the hosting capacity of renewable power generators, and to improve the energy security and reliability, while offering flexibility services to the grid. For these reasons, it is considered as one of the most promising enabling technologies for the large scale deployment of the Smart Grids (SGs) paradigm [5]. Aside from the available generation facilities, MGs are able to work in a double operating mode: islanded/stand-alone mode and grid-connected mode [6]. In grid-connected mode, the voltage and frequency of the MG are dictated by the main grid, while in islanded/stand-alone mode control units embedded within each DGs are responsible for frequency and voltage restoration, along with managing active and reactive power [7]. To face this issue, the most common approach is to deploy a three-layer hierarchical control architecture [8], which is based on the following interactive modules: *i*) a Primary Control (PC) level, commonly called zero-level, involving the local hardware control of each DG unit and designed to stabilize the power network, as well as to share active and reactive power among different distributed energy sources, without any communication links; *ii*) a Secondary Control (SC), properly designed in order to compensate inevitable voltage and frequency fluctuations caused by the operation of PC layer; *iii*) a Tertiary Control (TC) aimed at optimizing the power flows exchanged by the MG components [9]. Since PC induces unavoidable frequency and voltage deviation, the SC becomes essential for MG performances. In power transmission systems, a centralized secondary controller is typically adopted to give compensation signals to the PC, where a central computing unit periodically collects and processes the grid data, coordinating the operation of the available MG components, all used with the aim of minimizing the fluctuations of the load buses voltage magnitudes, improving the power quality, and reducing the imbalances of the programmed power profiles exchanged with the main electrical grid. This is obtained by solving an optimal power flow problem [10], which aims at minimizing a cost function given by the combination of different control objectives (voltage profile flattening, power losses, reactive power cost etc) in the presence of several constraints (reliability indexes, voltage stability limits etc) [11]. Unfortunately, the deployment of this centralized computing paradigm is not easily applicable in MGs. Unaffordable complexity, hardware redundancy, network bandwidth and data storage resources are the main barriers imposed by technology and costs. Moreover, as pointed out in [12], there are other mainly limitations in this approaches in terms of scalability and sensitivity to single-point failures, i.e. when a fault occurs in the central unit the whole system may collapse.

In this context, the MG community has identified the most promising research directions as: *a*) conceptualization of new automation and control paradigms for distribution of the intelligence at field level (e.g. delocalization of functions usually processed by the remote control centres); *b*) implementation of communications from MG components to remote centers but also among the distributed components at substation level (pervasive communication networks); *c*) use of international standards to improve interoperability.

Along this direction, Multi-Agent System (MAS) paradigm has been recognized as the most promising enabling technology for the designing of the SC layer [13]. According to this mathematical framework, each MG component is represented by a dynamic system which, sharing information with the neighboring agents, aims at achieving a common coordinated behavior at the global level via distributed control protocols [11], [14]. Leveraging this paradigm, the voltage/frequency restoration, as well as the power sharing control problems, for stand-alone MGs have been solved without considering communication impairments in [15], [16], which propose a distributed an event-triggered distributed controller, while [17], [18] present a nonlinear robust consensus-based strategy. Neglecting again communication delays, [19] proposes a distributed economic power dispatch and bus voltage control solution for droop-controlled DC MGs, while a coordination among the three control layers is discussed in [20] in order to realize a method for their joint operations.

Modelling communication impairments as a white noise, both linear and nonlinear consensus-based approach have been very recently addressed in [21]–[23]. However, in practise, when dealing with control of connected DG units leveraging wireless communication, also communication time delay into the shared information and sudden packet losses, originated by communication active links, naturally arise. Therefore the hypothesis of perfect and ideal communication among agents is not realistic, as well as the one of modeling impairments only via additive noises may be restrictive. Nevertheless, few papers address the presence of communication

time-delays in the MG control [24]. For example, a linear quadratic regulator have been exploited in [25] under the hypothesis of a unique constant time-delay. Along this direction, a robust neighbor-based distributed cooperative control strategy is proposed in [26] for DC MGs by considering slow switching topologies and a constant and homogeneous time delay for the overall communication network. However, in practice information shared via a wireless communication networks is affected by time-varying delays depending on the actual condition of the specific communication channel, thus making the assumption of unique delays too restrictive [27]. Considering communication delays as time-varying functions, [23], [28] have suggested a droop-based distributed cooperative control, but no delay-dependent gain-tuning rule has been provided. This implies that no stability margin w.r.t. delays, also larger than the typical average value of the end-to-end communication, can be guaranteed by the proposed controllers.

Furthermore, for practical MG management application, the control accuracy is crucial and hence, it is required that the convergence towards the desired behaviour should be reached in a finite-time [29]. Specifically, in MGs framework, a faster convergence rate is required by the presence of variable loads, that require nominal operating conditions in terms of both frequency and voltage magnitudes. Therefore, in this context it is crucial to guarantee voltage synchronization process occurs in finite-time [30]. To this aim, several finite-time control protocols are recommended in technical literature, both continuous and discontinuous (see e.g. [31], [32] and references therein).

The more challenging problem of designing a distributed control strategy, ensuring prescribed transient behaviour for the MG while coping with communication time-varying delays has sparsely been addressed. Along this line, the very recent work in [33] suggests a distributed finite-time control protocol, for frequency and voltage restoration, that also leverages the Artstein model reduction method for counteracting the unique constant delay affecting the communication network. A first attempt to solve, instead, this issue in the presence of time-varying communication delays can be found in [34], where the finite-time voltage control problem is solved via a distributed input-delayed control strategy.

Moreover, all the aforementioned finite-time or delay-dependent control strategies are validated in simplified simulation scenarios, where each bus is equipped with a DG and its corresponding local load, thus perfectly overlapping the electrical topology with the communication one. Nevertheless, this assumption may not to be realistic [25].

To tackle all these crucial aspects, this work suggests a novel robust networked-based finite-time controller under realistic conditions, where the electrical topology does not match with the communication one. The proposed controller acts by restoring the DGs voltages to reference set-points, while counteracting communication latency, arising from the information sharing, as well as both model mismatches and load changes occurring in real practical operative scenarios.

Therefore, the main contributions include the following:

- Unlike [22], [26], [35], our control approach ensures the finite-time stability of the MG, thus allowing both to speed-up the synchronization process to the reference behaviour despite the presence of sensitive loads and communication latencies and to guarantee prescribed transient performances;
- Differently from [22], [35], by exploiting Lyapunov-Krasovskii theory and Finite-Time stability tools, we provide a delay-dependent control gain tuning procedure, expressed as set of LMI, whose solution allows finding the voltage controller gain and state trajectories bound as function of the upper bound for the communication time-delay; this guarantees a certain stability margin w.r.t. sudden packet losses, which can be modeled as hard delays;
- Differently from [22], [28], [32], [35], an extensive simulation analysis is carried out by considering a practical case-of-study of the IEEE 14-bus Test system, where no overlapping between electrical and communication layers is considered. Moreover, the worst case scenarios of hard load variations and plug-and-play of DG units are also discussed in order to confirm the robustness of the proposed control approach with respect to sudden changing into the surrounding environment;
- The validation of the proposed networked-based finite-time delayed control action also in the IEEE 30 bus test system with more distributed energy resources corroborates its applicability on larger networks.

Note that some preliminary results have been presented in our previous work [34], but there neither the analytic derivation of control gain tuning procedure, nor the formulation of the problem and its validation in a realistic case have been addressed.

The paper is organized as follows. In Section II-A, the mathematical preliminaries are introduced. In Section III a model for the whole stand-alone MG is derived. The robust cooperative finite-time voltage SC is presented in Section IV, while its stability analysis and the related control gain tuning procedure are presented in Section V. The thorough simulation analysis, carried out on the IEEE 14-bus test systems, are disclosed in Section VI. Conclusions are drawn in Section VII.

II. MATHEMATICAL BACKGROUND

Some useful Definitions and preliminaries are reported in this section for the sake of clarity.

A. GRAPH THEORY

According to MAS framework, a power network can be modeled like a directed graph, defined as $\mathcal{G}_N = \{\mathcal{V}_N, \mathcal{E}_N\}$, where $\mathcal{V}_N = \{1, 2, \ldots, N\}$ is the set of vertices, i.e. the dynamical nodes, while $\mathcal{E}_N \subseteq \mathcal{V}_N \times \mathcal{V}_N$ is the set of edges, that mimic direct and active communication links. Hence, given two distinct nodes i and j, an edge from i to j defines

a pair $(i, j) \in \mathcal{E}_N$ and it represents information flow between the two nodes. In so doing, the weighted adjacency matrix $\mathcal{A} = [a_{ij}] \in \mathbb{R}^{N\times N}$ can be associated to the graph $\mathcal{G}_N$, whose element $a_{ij} \neq 0$ if there is an active communication link between agents j and i, i.e. $(i, j) \subseteq \mathcal{E}_N$, otherwise $a_{ij} = 0$. With this matrix, it is possible to define the Laplacian matrix as $\mathcal{L}$ such that $l_{ii} = \sum_{j\neq i}^{N} a_{ij}$ and $l_{ij} = -a_{ij}$ with $i \neq j$. Let $\mathcal{N}_i = \{j \in \mathcal{V}_N : (i, j) \in \mathcal{E}_N\}$ the neighboring set of the i-th node. If there exists a leader agent, usually labelled with index zero, i.e. node 0, the resulting network topology can be modeled via an augmented graph $\mathcal{G}_{N+1}$. Moreover, we can introduce the pinning matrix $\mathcal{P} = diag\{p_i\} \in \mathbb{R}^{N\times N}$ whose element p_i is equal to 1 when the leader sends its information to agent i via a direct communication link (i.e. the agent *is* is pinned to the leader), 0 otherwise [36]. Furthermore, according to [36] we define a directed path from node i to node j as a sequence of nodes that starts in i and ends in j, i.e. $(i, p), (p, q), \cdots, (r, j)$. Then, a generic agent $i \in \mathcal{G}_N$ is globally reachable if it can be reached through a directed path from any other node.

Through the paper, we model both the physical and communication network topologies via di-graphs.

B. FINITE-TIME STABILITY

Let a delayed system as

$$\dot{x}(t) = Ax(t) + Bx(t - \tau(t)) + Fw(t) \tag{1}$$

being $x(t) \in \mathbb{R}^N$ the state vector, $\tau(t)$ the time-varying delay due to the communication network such that $\tau(t) \in [0, \tau^\star]$, $\dot{\tau}(t) \in [0, \mu]$ with $\mu < 1$ [37]; $w(t) \in \mathbb{R}^N$ the bounded disturbances vector; and A, B, F known matrices of appropriate dimensions.

Definition 1 (Robust Finite-Time Stability for Time-Delay Systems [38], [39]): Given positive scalars T^f, $\tau^\star$, Π, c_1 and c_2 with $c_2 > c_1$ and a matrix $\Psi > 0$, system (1) is said to be robust finite-time stable (RFTS) with respect to $(c_1, c_2, \tau^\star, T^f, \Psi, \Pi)$ if

$$\sup_{-\tau^\star\leq t_0\leq 0} \{x^\top(t_0)\Psi x(t_0), \dot{x}^\top(t_0)\Psi\dot{x}(t_0)\} \leq c_1$$
$$\Longrightarrow x^\top(t)\Psi x(t) < c_2 \quad t \in [t_0, t_0 + T^f]$$

for all the disturbances $w(t)$ satisfying $\int_0^{T^f} w^\top(t)w(t) \leq \Pi$.

III. MICROGRID MODELLING

Let N and M the numbers of DGs and local loads within stand-alone MG. These entities are physically interconnected through power lines, while a communication layer is also included leading to an interaction among them in the cyber-space, thus guaranteeing the information sharing and the achieving of the SC aims (see Figure 1).

In what follows, to create a detailed framework, the problem formulation will be discussed starting from an accurate mathematical model for DGs and for the overall stand-alone MG network. Note that, according to the technical literature [40], Microgrid modeling can be categorized into two main classes: inverter-interfaced DG units [41] and the so-called small signal model [42]. Although in the former the model derivation is restricted to single DG, while the current and power flows between different units are non-explicitly considered, in the sequel we consider the inverter-based modelling since the future electrical networks will be composed of inverter-based electrical devices [40].

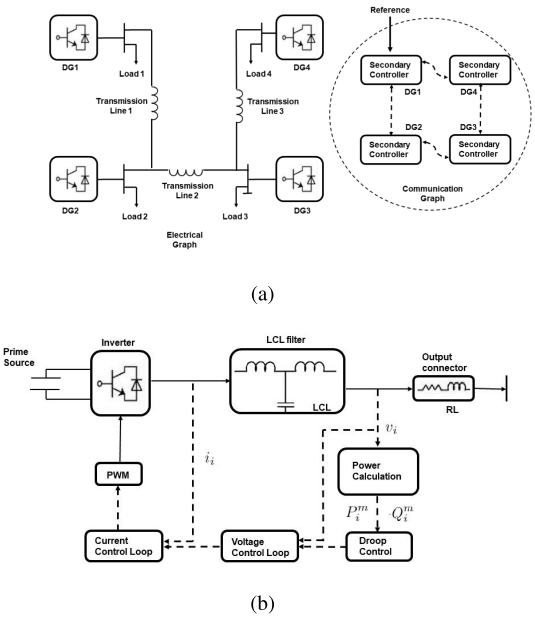

FIGURE 1. Exemplar inverter-based Microgrid: a) stand-alone MG consisting of four DGs and four loads; b) primary control block scheme.

A. DG MODEL

A PC layer is locally implemented in each inverter-based DG unit, consisting of three-phase dc/ac inverter, a dc source, RL output connector and an LCL filter [32]. Moreover, an inner voltage control loop and current control loop along with the power control are included in order to regulate the inverter voltage and current and to help power sharing task [43], thus reacting the instability phenomenon both in frequency and voltage magnitudes after PCC disconnection process [44].

Therefore, the dynamics of the i-the DG unit is expressed by the following approximated droop equations $(\forall i = 1, \ldots, N)$ as [45]:

$$\dot{\delta}_i = \omega_i = \omega^\star - k_{P_i}P_i^m + u_i^\omega, \tag{2a}$$
$$k_{v_i}\dot{v}_i = -v_i + v^\star - k_{Q_i}Q_i^m + u_i^V, \tag{2b}$$

being $v^\star$ and $\omega^\star$ the set-points for the voltage and frequency respectively, $k_{P_i} \in \mathbb{R}^+$ and $k_{Q_i} \in \mathbb{R}^+$ the droop gains, $k_{v_i} \in \mathbb{R}^+$ the voltage control gain, while the inputs for the secondary frequency and voltage control are u_i^ω and u_i^V, respectively. Note that $u_i^\omega = u_i^V = 0$ means that SC is inactive.

Moreover, the measured real and reactive power, i.e. P_i^m and Q_i^m respectively, are given via the following first-order low-pass filter [32]:

$$\tau_{P_i}\dot{P}_i^m = -P_i^m + P_i, \tag{3a}$$
$$\tau_{Q_i}\dot{Q}_i^m = -Q_i^m + Q_i, \tag{3b}$$

where τ_{P_i} and τ_{Q_i} are the filter time constants, P_i and Q_i are the active and reactive power outputs of the i-th DG.

B. MG NETWORK MODEL

The communication layer describing the information exchange among the smart controllers associated with each DG i, $\forall i = 1, \ldots, N$ whitin the MG in the cyber-physical space can be modeled according to graph theory. Specifically, we consider N DG units together with a leader agent, taken as an additional node labelled with index zero (i.e. node 0), which provides the reference behaviours for both voltage and frequency (v_0, ω_0) in order to achieve SC objectives. Indeed, the leader node can broadcast this set-point $(v_0, \omega_0) \in \mathbb{R}$ to a subset of DGs smart controllers. To this aim, we use an augmented directed graph $\mathcal{G}_{N+1}^c = \{\mathcal{V}_{N+1}^c, \mathcal{E}_{N+1}^c, \mathcal{A}^c\}$ to model the resulting network topology, where $\mathcal{V}_{N+1}^c$ is the set embedding the DGs and the leader node, while $\mathcal{E}_{N+1}^c$ is the set of edges that describes the communication links. In this way, the communication structure can be described by the corresponding adjacency matrix $\mathcal{A}^c = [a_{ij}] \in \mathbb{R}^{(N+1)\times(N+1)}$, whose generic element $a_{ij} = 1$ if there is a communication link from node j to node i, 0 otherwise. By defining the leader node 0 globally reachable in $\mathcal{G}_{N+1}^c$ if there exists a path from every DGs node i, $\forall i = 1, \ldots, N$ to leader node 0, throughout this paper we assume the global reachability property for the leader agent.

Moreover, note that, in real communication network, time-varying communication delays might arise during the information sharing process among different agent, whose value depends on the current availability of the wireless channel itself. Therefore, in order to avoid and prevent any instability phenomenon, the presence of this delay $\tau(t)$ affecting the set of the edges $\mathcal{E}_{N+1}^c$ has to be considered during control design phase [27]. Finally, $\mathcal{N}_i^c = \{j : (i, j) \in \mathcal{E}_{N+1}^c\}$ denotes the neighboring set of the DG unit i, $\forall i = 1, \ldots, N$.

Besides the communication network topology, in order to deal with the problem, it is necessary to introduce an electrical network topology to characterize the physical interconnection among the $N + M$ electric entities (i.e. the N DGs and the M local loads), which is allowed via power lines (see Fig.1 (a)). To this aim, by leveraging graph theory, we introduce a directed graph $\mathcal{G}_{N+M}^e = \{\mathcal{V}_{N+M}^e, \mathcal{E}_{N+M}^e, \mathcal{A}^e\}$, being $\mathcal{V}_{N+M}^e$ the electrical entities set and $\mathcal{E}_{N+M}^e$ the set of the electric edges, i.e. the impedences of the power lines. Indeed, $\mathcal{A}^e$ represent the adjacency matrix associated to the electrical topology, whose complex weight are the admittance between different buses. For example, the generic $a_{\rho k} = Y_{\rho k} = G_{\rho k} + jB_{\rho k}$, being $Y_{\rho k} \in \mathbb{C}, G_{\rho k} \in \mathbb{R}$ and $B_{\rho k} \in \mathbb{R}$ the admittance, the conductance and susceptance, respectively. $Y_{\rho k} = 0$ means that does not exists a power line between the ρ-th and the k-th bus. Similarly, we can introduce $\mathcal{N}_\rho^e = \{k : k \in \mathcal{V}_{N+M}^e, k \neq \rho, Y_{\rho k} \neq 0\}$, i.e. the set of neighbors of the ρ-th electrical unit. In addition, we have $G_{\rho\rho} = \sum_{k\in\mathcal{N}_\rho^e} G_{\rho k}$ and $B_{\rho\rho} = \sum_{k\in\mathcal{N}_\rho^e} B_{\rho k}$.

Note that, this kind of representation for the communication and the electrical layers is possible according to the appraised inverter-based MG modelling [40]. Hereinafter some useful and common assumption are given [7].

Assumption 1: The power transmission lines within the MG, describing the electrical network topology $\mathcal{G}_{N+M}^e$, are lossless. This implies that the conductance is always zero, i.e. $G_{\rho k} = 0$, and $Y_{\rho k} = jB_{\rho k}, \forall \rho \in \mathcal{V}_{M+M}, k \in \mathcal{N}_\rho^e$.

Note that, the above assumption is common and reasonable in power system analysis (see e.g. [46], [47] and references therein). Indeed, the lossless line admittance may be justified as follows: in MV and LV networks the line impedance is usually not purely inductive, but has a non-negligible resistive part. On the other hand,the inverter output impedance is typically inductive(due to the output inductance and/or the possible presence of an output transformer). Under these circumstances, the inductive parts dominate the resistive parts [46]. Moreover, Assumption 1 is also crucial for control design phase. Indeed, by considering dominant inductive networks, the influence of the dynamics of the phase angles on the reactive power flows can be neglected [48].

Taking into account the above Assumption 1 together with the power balance equations [49], the following relations hold:

$$\hat{P}_\rho = \sum_{k\in\mathcal{N}_\rho^e} v_\rho v_k B_{\rho k} \sin(\delta_\rho - \delta_k), \tag{4a}$$
$$\hat{Q}_\rho = v_\rho^2 B_{\rho\rho} - \sum_{k\in\mathcal{N}_\rho^e} v_\rho v_k B_{\rho k} \cos(\delta_\rho - \delta_k), \tag{4b}$$

being $\hat{P}_\rho$, $\hat{Q}_\rho$, v_ρ and δ_ρ the active injected power, the reactive injected power, the measured voltage and phase angle of the bus ρ, $\forall \rho \in \mathcal{V}_{N+M}^e$, respectively.

Moreover, to integrate the presence of a local load within a specific bus ρ, we refer to the so-called ZIP load model expressed as [50]

$$P_{L_\rho} = P_{1_\rho} v_\rho^2 + P_{2_\rho} v_\rho + P_{3_\rho}, \tag{5a}$$
$$Q_{L_\rho} = Q_{1_\rho} v_\rho^2 + Q_{2_\rho} v_\rho + Q_{3_\rho}, \tag{5b}$$

where the pair (P_{1_ρ}, Q_{1_ρ}) represents the nominal constant impedence loads, (P_{2_ρ}, Q_{2_ρ}) indicates the pair for the nominal constant current loads, while (P_{3_ρ}, Q_{3_ρ}) the ones related to nominal constant power loads.

Putting together (4)-(5), we can have:

$$P_i = \sum_{\rho\in\mathcal{N}_i^e} P_{L_\rho} + \sum_{\rho\in\mathcal{N}_i^e} \hat{P}_\rho, \tag{6a}$$
$$Q_i = \sum_{\rho\in\mathcal{N}_i^e} Q_{L_\varepsilon} + \sum_{\rho\in\mathcal{N}_i^e} \hat{Q}_\rho, \tag{6b}$$

where P_i and Q_i are the total active and reactive power output of the DG i, $\forall i = 1, \ldots, N$.

Assumption 2: There exist prescribed known constants $\Pi^Q, \Pi^P \in \mathbb{R}^+$ *such that*

$$|Q_i| \leq \Pi^Q, \ |P_i| \leq \Pi^P \ \ \forall i.$$

This ensures that reactive and active power (6b) and (6a), as well as (3b) and (3a), are bounded.

Remark 1: Assumption 2 is reasonable in power system since, by considering a fixed operating point of the inverter, the magnitudes of these powers do not exceed their tresholds, thus preventing any instability conditions [32].

Remark 2: Since frequency and voltage control design phases are commonly decoupled, we discuss frequency and voltage controllers separately (see [30] and references therein).

Therefore, the focus of the work is to suggest a novel robust delayed finite-time cooperative networked-based control protocol able to ensure accurate voltage trajectory tracking of the leader node by the DGs within the MG despite the presence of time-varying communication latency. To increse the clarity of the work, in the next section we present a well-known frequency controller proposed in [7], used to implement a real case-of-study ans to test our voltage control protocol.

C. FREQUENCY CONTROLLER

The frequency SC objective is to achieve real power sharing condition and to synchronize the DGs frequency to the reference value ω_0, i.e. $\lim_{t\to\infty} \omega_i(t) = \omega_0$, taking into account the control input frequency constraints expressed as $(u_i^\omega)_s/(u_j^\omega)_s = 1, \ i \neq j \in \mathcal{V}_{N+1}^c - \{0\}$, where $(u_i^\omega)_s$ and $(u_j^\omega)_s$ are the frequency control input of the i-th and j-th DG within the MG in steady state conditions. The achievement of this control goal is guaranteed under the following distributed control strategy [7]:

$$\begin{aligned} u_i^\omega &= \alpha_i(\hat{\omega}_i - \omega_i) \\ \dot{\hat{\omega}}_i &= \beta_i \sum_{j\in\mathcal{N}_i^c} (\omega_i - \omega_j) + g_i(\omega_i - \omega_0) + \varphi_i \sum_{j\in\mathcal{N}_i^c} (u_j^\omega - u_i^\omega) \end{aligned} \tag{7}$$

being $\alpha_i, \beta_i, \varphi_i \in \mathbb{R}^+$ the proper tuned control gains, while g_i models the communication links between the DGs and the leader node (see Section III-B).

IV. DISTRIBUTED COOPERATIVE FINITE-TIME VOLTAGE CONTROL PROTOCOL IN THE PRESENCE OF COMMUNICATION DELAYS

The aim of this section is to handle with the problem of voltage restoration arising at secondary control level in inverter-based stand-alone MG, i.e. to guarantee that all the DGs within the MG track the reference behaviour as imposed by the leader node, indexed with 0. Specifically, we design a finite-time control strategy meant to be distributed, i.e. it has to induce a common required behaviour for the overall network of DGs, that is also able to counteract time-varying communication latency arising from the information exchange. To deal with the above problem, the control objective is to design a distributed networked-based delayed strategy $u_i^V(t, \tau(t))$ such that:

- $\|v_i(t) - v_0(t)\| \to 0$ as $t \to T^f$, being v_i, v_0, T^f the voltage of i-th DG within the MG, the voltage set-point and desired settling time respectively;
- there exists constant $c_2 \in \mathbb{R}^+$ acting as a threshold for all voltage error trajectories w.r.t. the reference voltage set-point within each transient time interval $[t, t + T^f]$.

The voltage leader dynamic is given by the following differential equation:

$$\dot{x}_0(t) = Ax_0(t) \tag{8}$$

where $x_0(t) = \begin{bmatrix} v_0(t) & \dot{v}_0(t) \end{bmatrix} \in \mathbb{R}^2$ is the state vector of the leader.

To put the DG voltage dynamic into state-space form, we differentiate (2b) as:

$$k_{v_i}\ddot{v}_i(t) + \dot{v}_i(t) - k_{Q_i}\dot{Q}_i^m(t) + u_i^V(t, \tau(t)) = 0, \tag{9}$$

being u_i^V the cooperative SC input for voltage regulation computed by leveraging the outdated information shared via communication links, described by $\mathcal{G}_{N+1}^c$, due to communication latency [51]. Indeed, in order to avoid instability phenomenon, it is necessary to consider communication time-delays $\tau(t)$ from the control design phase. Finally, Eq. (9) can be rewritten as

$$\dot{x}_i(t) = Ax_i(t) + B_i u_i^V(t, \tau(t)) + G_i w_i(t). \tag{10}$$

Note that, Eq. (10) is a delayed-input system, where $x_i(t) = [v_i(t) \ \ \dot{v}_i(t)]^\top$ is the state vector; $w_i(t) = [0, \ \ (-\dot{v}_i(t) - k_{Q_i}\dot{Q}_i^m(t))]^T$ is the time-varying disturbance vector that take into account the voltage deviation induced by droop-PC, while A, B_i, and G_i are

$$A = \begin{bmatrix} 0 & 1 \\ 0 & 0 \end{bmatrix}, \ B_i = G_i = \begin{bmatrix} 0 \\ \dfrac{1}{k_{v_i}} \end{bmatrix},$$

respectively. In addition, Assumption 2 and Remark 2 guarantee that

$$\exists \quad \Pi \in \mathbb{R}^+ : |w_i(t)| \leq \Pi, \tag{11}$$

which means that the disturbances are bounded. The achievement of the aforementioned control objectives is guaranteed under the following distributed delayed finite-time control strategy:

$$u_i^V(t, \tau(t)) = K \sum_{j\in\mathcal{N}_i^c} a_{ij}\big(x_i(t - \tau(t)) - x_j(t - \tau(t))\big), \tag{12}$$

where $K \in \mathbb{R}^{1\times 2}$ is the control gains vector to be proper tuned; coefficient a_{ij}, as defined in Section II-A), model the communication network topology emerging from the presence/absence of a communication link between the DG i and DG j in the SC level; $\tau(t)$ is the communication time-varying

latency which is detectable by timestamp. Note that, the presence of $\tau(t)$ over the network leads to the need of running the controller on the basis of outdated information as in (12).

We highlight that the proposed control protocol in (12) is homogeneous and continuous, thus allowing to prevent chattering phenomenon arising from discontinuous control law [52].

V. FINITE-TIME STABILITY ANALYSIS

In this section, we provide the stability conditions guaranteeing the robust finite-time voltage regulation problem in a MG despite the presence of communication delay. This conditions are expressed as a set of LMIs, whose solution also allows finding the suitable control gains vector $K \in \mathbb{R}^{1\times 2}$ in (12).

To this aim, we first derive the mathematical representation of the MG closed-loop system under the action of the distributed control (12). Hence, given the dynamics of DG i in (10) and the ones of the leading agent as in (8), we define the error vector for each DG i w.r.t. to the leader as

$$e_i(t) = x_i(t) - x_0(t) \qquad \forall i \in \mathcal{V}^c_{N+1} - \{0\}.$$

According to the above definition and considering the control input u_i^V as in (12), it is possible to derive the closed-loop error dynamics for the i-th DG as

$$\dot{e}_i(t) = Ae_i(t) + B_iK \sum_{j\in\mathcal{N}_i^c} a_{ij}(e_i(t-\tau(t)) - e_j(t-\tau(t))) + G_iw_i(t). \quad (13)$$

Now, in order to describe the closed-loop network for the overall MG in a more compact form, by taking into account the communication topology, we define the augmented state vector $\tilde{x}(t) = [e_1^\top(t), e_2^\top(t), \cdots, e_N^\top(t)]^\top \in \mathbb{R}^{2N\times 1}$ and the augmented disturbance vector $\bar{w}(t) = [w_1^\top(t), w_2^\top(t), \cdots, w_N^\top(t)] \in \mathbb{R}^{2N\times 1}$, thus obtaining the following delayed closed-loop system:

$$\dot{\tilde{x}}(t) = \bar{A}\tilde{x}(t) + A_\tau\tilde{x}(t-\tau(t)) + G\bar{w}(t), \quad (14)$$

where $\bar{A} = (I_N \otimes A)$; $A_\tau = \sum_i(\mathcal{H}\otimes B_iK)$; $G = \sum_i(I_N \otimes G_i)$ where $\otimes$ is the Kronecker product and $\mathcal{H} = \mathcal{L} + \mathcal{P}$, being $\mathcal{L}$ and $\mathcal{P}$ the Laplacian and Pinning matrices of the graph $\mathcal{G}^c_{N+1}$.

The following common assumption related to communication time delay holds [53].

Assumption 3: [37] The homogeneous time-varying communication delay $\tau(t)$ is bounded, i.e. $\tau(t) \in [0, \tau^\star]$ and $\dot{\tau}(t) \in [0, \mu[$ with $\tau^\star$ and $\mu < 1 \in R^+$.

Now, we derive the sufficient conditions that guarantee the robust finite-time stability of the closed-loop dynamical system (14) according to the theorem stated as follows.

Theorem 1: Consider the closed-loop MG network as in (14) and let Assumption 3 holds. Given positive scalars α, T_f, Π, c_1, $c_2 > c_1$ and positive matrix $\Psi \in \mathbb{R}^{2N}$, let free matrices M, $T \in \mathbb{R}^{2N}$ and free-invertible matrix $F \in \mathbb{R}^{2N}$, being $F^{-1} = X$. Assume there exist a positive constant γ and positive matrices $P, Q, Z \in \mathbb{R}^{2N}$, $\bar{Q} = \Psi^{\frac{-1}{2}}Q\Psi^{\frac{-1}{2}}$ and $\bar{Z} = \Psi^{\frac{-1}{2}}Z\Psi^{\frac{-1}{2}}$ such that:

$$\begin{bmatrix} \Sigma_{11} & -M^\top + T & -A_\tau - M^\top & \bar{A}^\top & G \\ \star & -Q(1-\mu)e^{\alpha\tau^\star} - T^\top - T & -T & -A_\tau^\top & 0 \\ \star & \star & -Z & 0 & 0 \\ \star & \star & \star & \tau^{\star 2}P + X^\top + X & -G \\ \star & \star & \star & \star & \gamma I \end{bmatrix} < 0, \quad (15)$$

$$e^{\alpha T^f}\left(1 + \lambda_{max}(\bar{Q})\tau^\star + \lambda_{max}(\bar{Z})\frac{\tau^{\star 2}}{2}\right)c_1 + \gamma\Pi e^{\alpha T^f} < c_2, \quad (16)$$

being $\Sigma_{11} = (\bar{A} + A_\tau) + (\bar{A} + A_\tau)^\top + Q + M + M^\top - \alpha I$, $\lambda_{max}(\cdot)$ and $\lambda_{min}(\cdot)$ the maximum and minimum eigenvalues of matrices $\bar{Q}$ and $\bar{Z}$, respectively. Then system (14) is robust finite-time stable with respect to $(c_1, c_2, \tau^\star, T^f, \Psi, \Pi)$ for all the disturbances satisfying (11).

Proof: Consider the following Lyapunov-Krasovskii functional:

$$V(\tilde{x}(t)) = V_1(\tilde{x}(t)) + V_2(\tilde{x}(t)) + V_3(\tilde{x}(t)) \quad (17)$$

where

$$V_1(\tilde{x}(t)) = \tilde{x}^\top(t)\tilde{x}(t); \quad (18)$$

$$V_2(\tilde{x}(t)) = \int_{t-\tau(t)}^{t} \tilde{x}^\top(s)e^{\alpha(t-s)}Q\tilde{x}(s)\,ds; \quad (19)$$

$$V_3(\tilde{x}(t)) = \tau^\star\int_{-\tau^\star}^{0}\int_{t+\theta}^{t} \dot{\tilde{x}}^\top(s)e^{\alpha(t-s)}Z\dot{\tilde{x}}(s)\,ds\,d\theta \quad (20)$$

being Q and Z some symmetric and positive definite matrices.

Differentiating $V_1(\tilde{x}(t))$ in (18) along the trajectories of the closed-loop system (14), we have:

$$\begin{aligned}\dot{V}_1(\tilde{x}(t)) &= \dot{\tilde{x}}^\top(t)\tilde{x}(t) + \tilde{x}(t)^\top\dot{\tilde{x}}(t) = 2\tilde{x}^\top(t)\dot{\tilde{x}}(t) \\ &= 2\tilde{x}^\top(t)\bar{A}\tilde{x}(t) + 2\tilde{x}^\top(t)A_\tau\tilde{x}(t-\tau(t)) \\ &\quad + 2\tilde{x}^\top(t)G\bar{w}(t). \end{aligned} \quad (21)$$

By leveraging the Newton-Leibnitz formula [37]

$$\tilde{x}(t-\tau(t)) = \tilde{x}(t) - \int_{t-\tau(t)}^{t}\dot{\tilde{x}}(s)\,ds,$$

the equality (21) can be rewritten as:

$$\dot{V}_1(\tilde{x}(t)) = \tilde{x}^\top(t)(\Phi + \Phi^\top)\tilde{x}(t) - 2\tilde{x}^\top A_\tau\int_{t-\tau(t)}^{t}\dot{\tilde{x}}(t)\,ds + 2\tilde{x}^\top(t)G\bar{w}(t) \quad (22)$$

being $\Phi = \bar{A} + A_\tau$.

Moreover, given Assumption 3, by differentiating $V_2(\tilde{x}(t))$ in (19) and $V_3(\tilde{x}(t))$ in (20) along the trajectories of (14), it yields:

$$\dot{V}_2(\tilde{x}(t)) \le \tilde{x}^\top(t)Q\tilde{x}(t) - \tilde{x}^\top(t-\tau(t))e^{\alpha\tau^\star}Q(1-\mu)\tilde{x}(t-\tau(t)) + \alpha V_2(\tilde{x}(t)), \quad (23)$$

$$\begin{aligned}\dot{V}_3(\tilde{x}(t)) &\leq \tau^{\star 2}\dot{\tilde{x}}^\top(t)Z\dot{\tilde{x}}(t) - \int_{t-\tau(t)}^{t}\dot{\tilde{x}}^\top(s)e^{\alpha(t-s)}Z\dot{\tilde{x}}(s)\,ds \\ &\quad + \alpha V_3(\tilde{x}(t)) \\ &\leq \tau^{\star 2}\dot{\tilde{x}}^\top(t)Z\dot{\tilde{x}}(t) - \int_{t-\tau(t)}^{t}\dot{\tilde{x}}^\top(s)Z\dot{\tilde{x}}(s)\,ds \\ &\quad + \alpha V_3(\tilde{x}(t)). \end{aligned} \tag{24}$$

By applying Jensen inequality [37] on the integral term of inequality (24), it follows:

$$\begin{aligned}\dot{V}_3(\tilde{x}(t)) &\leq \alpha V_3(\tilde{x}(t)) + \tau^{2\star}\dot{\tilde{x}}(t)Z\dot{\tilde{x}}(t) \\ &\quad -\left(\int_{t-\tau(t)}^{t}\dot{\tilde{x}}(s)\,ds\right)^\top Z\left(\int_{t-\tau(t)}^{t}\dot{\tilde{x}}(s)\,ds\right). \end{aligned} \tag{25}$$

Finally, summing up (22), (23) and (25), we obtain:

$$\begin{aligned}\dot{V}(\tilde{x}(t)) &\leq \tilde{x}^\top(t)(\Phi+\Phi^\top)\tilde{x}(t) - 2\tilde{x}^\top A_\tau\int_{t-\tau(t)}^{t}\dot{\tilde{x}}(t)\,ds \\ &\quad + 2\tilde{x}^\top(t)G\bar{w}(t) + \tilde{x}^\top(t)Q\tilde{x}(t) \\ &\quad - \tilde{x}^\top(t-\tau(t))e^{\alpha\tau^\star}Q(1-\mu)\tilde{x}(t-\tau(t)) \\ &\quad + \alpha V_2(\tilde{x}(t)) + \alpha V_3(\tilde{x}(t)) + \tau^{2\star}\dot{\tilde{x}}^\top(t)Z\dot{\tilde{x}}(t) \\ &\quad -\left(\int_{t-\tau(t)}^{t}\dot{\tilde{x}}^\top(s)\,ds\right)^\top Z\left(\int_{t-\tau(t)}^{t}\dot{\tilde{x}}(s)\,ds\right). \end{aligned} \tag{26}$$

Now, we leverage the Free Matrices method [54], i.e.

$$\begin{aligned}&2\left(\tilde{x}^\top(t)M^\top + \tilde{x}^\top(t-\tau(t))T^\top\right) \\ &\qquad\times\left[\tilde{x}(t) - \tilde{x}(t-\tau(t)) - \int_{t-\tau(t)}^{t}\dot{\tilde{x}}(s)\,ds\right] = 0 \end{aligned} \tag{27}$$

and

$$2\dot{\tilde{x}}^\top(t)F^\top\left(\dot{\tilde{x}}(t) - \bar{A}\tilde{x}(t) - A_\tau\tilde{x}(t-\tau(t)) - G\bar{w}(t)\right) = 0, \tag{28}$$

being M, T and $F \in \mathbb{R}^{2N\times 2N}$ free matrices.

Summing the null terms (27) and (28) to the right-side of inequality (26), we obtain:

$$\begin{aligned}\dot{V}(\tilde{x}(t)) &\leq \tilde{x}^\top(t)\left(\Phi+\Phi^\top+Q+M+M^\top\right)\tilde{x}(t) \\ &\quad + 2\tilde{x}^\top(t)\left(M^\top+T\right)\tilde{x}(t-\tau(t)) + 2\tilde{x}^\top(t)G\bar{w}(t) \\ &\quad - 2\tilde{x}^\top(t)\left(A_\tau+M^\top\right)\int_{t-\tau(t)}^{t}\dot{\tilde{x}}(s)\,ds \\ &\quad + \tilde{x}^\top(t-\tau(t))\left(-Q(1-\mu)e^{\alpha\tau^\star}+T^\top\right. \\ &\quad \left.+T\right)\tilde{x}(t-\tau(t)) - 2\tilde{x}^\top(t-\tau(t))T^\top\int_{t-\tau(t)}^{t}\dot{\tilde{x}}(s)\,ds \\ &\quad + \dot{\tilde{x}}^\top(t)\left(\tau^{2\star}Z+F^\top+F\right)\dot{\tilde{x}}(t) - 2\dot{\tilde{x}}^\top(t)F^\top\bar{A}\tilde{x}(t) \\ &\quad - 2\dot{\tilde{x}}^\top(t)F^\top A_\tau\tilde{x}(t-\tau(t)) - 2\dot{\tilde{x}}^\top(t)F^\top G\bar{w}(t) \\ &\quad -\left(\int_{t-\tau(t)}^{t}\dot{\tilde{x}}^\top(s)\,ds\right)^\top Z\left(\int_{t-\tau(t)}^{t}\dot{\tilde{x}}(s)\,ds\right) \\ &\quad + \alpha V_2(\tilde{x}(t)) + \alpha V_3(\tilde{x}(t)). \end{aligned} \tag{29}$$

Now, by defining the following enlarged state vector:

$$\eta(t) = \left[\tilde{x}^\top(t)\ \tilde{x}^\top(t-\tau(t))\ \int_{t-\tau(t)}^{t}\dot{\tilde{x}}(s)\,ds\ \dot{\tilde{x}}^\top(t)\ \bar{w}(t)\right]^\top, \tag{30}$$

being $\eta(t) \in \mathbb{R}^{\nu\times\nu}$ with $\nu = 5\cdot 2N$, the inequality (29) can be recast into a more compact form as

$$\dot{V}(\tilde{x}(t)) \leq \eta^\top(t)\Xi\eta(t) + \alpha V_2(\tilde{x}(t)) + \alpha V_3(\tilde{x}(t)) \tag{31}$$

where

$$\Xi = \begin{bmatrix} \Xi_{11} & \Xi_{12} & \Xi_{13} & \Xi_{14} & \Xi_{15} \\ \star & \Xi_{22} & \Xi_{23} & \Xi_{24} & \Xi_{25} \\ \star & \star & \Xi_{33} & \Xi_{34} & \Xi_{35} \\ \star & \star & \star & \Xi_{44} & \Xi_{45} \\ \star & \star & \star & \star & \Xi_{55} \end{bmatrix} \in \mathbb{R}^{\nu\times\nu}, \tag{32}$$

being

$$\begin{aligned}&\Xi_{11} = \Phi+\Phi^\top+Q+M^\top+M, \quad \Xi_{12} = -M^\top+T, \\ &\Xi_{13} = -A_\tau - M^\top, \quad \Xi_{14} = \bar{A}^\top F, \quad \Xi_{15} = G, \\ &\Xi_{22} = -Q(1-\mu)e^{\alpha\tau^\star} - T^\top - T, \quad \Xi_{23} = -T^\top, \\ &\Xi_{24} = -A_\tau^\top F, \quad \Xi_{33} = -Z, \quad \Xi_{44} = \tau^{2\star}Z + F^\top + F, \\ &\Xi_{45} = -F^\top G, \quad \Xi_{25} = \Xi_{34} = \Xi_{35} = \Xi_{55} = 0_{2N\times 2N}. \end{aligned}$$

Summing and subtracting the terms $\alpha V(\tilde{x}(t))$ and $\gamma\bar{w}^\top(t)\bar{w}(t)$ to (31), after some algebraic manipulations we obtain:

$$\dot{V}(\tilde{x}(t)) - \alpha V(\tilde{x}(t)) \leq \eta^\top(t)\Xi'\eta(t) + \gamma\bar{w}^\top(t)\bar{w}(t), \tag{33}$$

being Ξ' as in (34), as shown at the bottom of the page. Choosing positive definitive matrices Q and $Z \in R^{2N}$, free matrices M, T, $F \in R^{2N\times 2N}$ and $\mathcal{L}_2$ gain γ such that the inequality in (34) is fulfilled, from (33) it follows:

$$\dot{V}(\tilde{x}(t)) - \alpha V(\tilde{x}(t)) \leq \gamma\bar{w}^\top(t)\bar{w}(t). \tag{35}$$

$$\Xi' = \begin{bmatrix} \Phi+\Phi^\top+Q+M^\top+M-\alpha I_{2N} & -M^\top+T & -A_\tau-M^\top & \bar{A}^\top F & G \\ \star & -Q(1-\mu)e^{\alpha\tau^\star}-T^\top-T & -T^\top & -A_\tau^\top F & 0_{2N\times 2N} \\ \star & \star & -Z & 0_{2N\times 2N} & 0_{2N\times 2N} \\ \star & \star & \star & \tau^{2\star}Z+F^\top+F & -F^\top G \\ \star & \star & \star & \star & -\gamma I_{2N} \end{bmatrix} < 0 \tag{34}$$

Then, for all $t \in [t_0, t_0 + T^f]$, being T^f the pre-fixed settling time, it holds:

$$V(\tilde{x}(t)) \leq e^{\alpha t} V(\tilde{x}(0)) + \gamma \int_0^t \bar{w}^\top(s)\bar{w}(s)\, ds \leq e^{\alpha T^f} V(\tilde{x}(0)) + \gamma \int_0^{T^f} \bar{w}^\top(s)\bar{w}(s)\, ds. \quad (36)$$

Now, in order to evaluate $V(\tilde{x}(0))$, we introduce the following relations:

$$\bar{Q} = \Psi^{\frac{-1}{2}} Q \Psi^{\frac{-1}{2}}, \quad \bar{Z} = \Psi^{\frac{-1}{2}} Z \Psi^{\frac{-1}{2}},$$

being $\Psi \in R^{2N}$ any positive matrix, i.e. $\Psi > 0$.

Given the above definitions, according to the choice of the Lyapunov-Krasovskii functional (17), after some algebraic manipulations we obtain:

$$\begin{aligned} V(\tilde{x}(0)) &= \tilde{x}^\top(0)\tilde{x}(0) + \int_{-\tau(0)}^{0} \tilde{x}^\top(s) e^{-\alpha s} Q \tilde{x}(s)\, ds \\ &\quad + \tau^\star \int_{-\tau^\star}^{0} \int_{\theta}^{0} \dot{\tilde{x}}^\top(s) e^{-\alpha s} Z \dot{\tilde{x}}(s)\, ds\, d\theta \\ &\leq \{1 + \lambda_{max}(\bar{Q})\tau^\star + \frac{\tau^{\star 3}}{2}\lambda_{max}(\bar{Z})\} \times \\ &\quad \sup_{-\tau^\star \leq t_0 \leq 0} \{\tilde{x}^\top(t_0)\Psi\tilde{x}(t_0);\ \dot{\tilde{x}}^\top(t_0)\Psi\dot{\tilde{x}}(t_0)\}. \quad (37) \end{aligned}$$

Given (37) and the boundedness of the disturbance vector as in (11), inequality (36) finally becomes:

$$V(\tilde{x}(t)) \leq e^{\alpha T^f}\left(1 + \lambda_{\max}(\bar{Q})\tau^\star + \lambda_{max}(\bar{Z})\frac{\tau^{\star 3}}{2}\right)c_1 + \gamma \Pi e^{\alpha T^f}, \quad (38)$$

being Π the maximum value of $\bar{w}(t)$ for all the domains that include the MG operation point.

Furthermore, from (17) we also have

$$V(\tilde{x}(t)) \geq \tilde{x}^\top(t)\tilde{x}(t) \geq \lambda_{min}(I)\tilde{x}^\top(t)\Psi\tilde{x}(t). \quad (39)$$

Finally, from (38) and (39) it follows:

$$\tilde{x}^\top(t)\Psi\tilde{x}(t) \leq e^{\alpha T^f}\left(1 + \lambda_{max}(\bar{Q})\tau^\star + \lambda_{max}(\bar{Z})\frac{\tau^{\star 3}}{2}\right)c_1 + \gamma \Pi e^{\alpha T^f} \leq c_2. \quad (40)$$

Therefore, if the inequality (34) and the LMI (16) hold, we have that the delayed closed-loop system (14) is robust finite-time stable according to Definition 1.

However, inequality (34) is not easy to solve since it is non-linear due to the presence of products between the matrix variable A_τ, depending on the control gains as in (12), and the other matrices variables. Hence, for effectively dealing with it, we exploit congruence transformation LMI property [55], thus transforming (34) into an equivalent LMI by pre- and post-multiply it with the matrix $\Upsilon = diag\{I, I, I, X, I\}$ and its transpose. In so doing, by defining $X = F^{-1}$ and $P = X^\top Z X$, after some algebraic manipulation, (34) is transformed into the LMI (15) depending on the linear combination of the controller gains. This completes the proof. □

Remark 3: The feasibility of the LMIs problem in (15)-(16) can be numerically verified by using, for example, the interior-point method [55] implemented in the Yalmip Toolbox with SeDuMi solver [56].

Remark 4: Since Finite-time control strategies can guarantee both a faster convergence than asymptotically ones and a best features in the presence of disturbances and uncertainties [29], it is particularly suitable adopt them in practical application like MGs control. Indeed, by reaching the voltage synchronization of all the DG units to the reference values in finite-time, the variable loads, which require nominal operating conditions, can be properly managed, thus allowing a proper disturbances rejection [30].

Remark 5: Feasible delay-dependent Matrix Inequalities in (15) and (16) are obtained through Theorem 1, which guarantee the robust finite-time voltage synchronization of the overall MG in (14). By fixing the maximum value $\tau^\star$ for the time delays, the value of c_1, Π (usually prescribed in technical literature [57]) and the couple (T^f, α), which force the overall performances of the entire MG in terms of settling time, thus conditioning state trajectories evolution and their threshold c_2, Eqs. (15) and (16) can be seen as Linear Matrix Inequalities. In so doing, the feasibility of the LMIs allows tuning the robust controller gains which guarantee the control objectives achievement despite the presence of communication latency, i.e. i) the voltage synchronization to the set-point in a finite-time T^f and ii) the boundedness of the state trajectories during each transient phase, being c_2 the threshold obtained via LMIs resolution.

Remark 6: When solving the LMIs in (15) and (16), we set an upper bound for communication delay $\tau^\star$, which is considered greater than the conventional threshold of the wireless communication network in normal operating conditions, e.g. based on the IEEE 802.11 protocol. Note that, hard delays, larger than the typical upper bound allowed by the wireless network, correspond to sudden packet losses. In doing so, the proposed procedure provides a meaningful robust stability margin with respect to the unavoidable latencies that can affect the networked cyber-physical system during some operative conditions. [27].

VI. PERFORMANCE ANALYSIS

In this section the effectiveness of the control approach is verified for the voltage regulation problem in the IEEE 14-bus test system depicted in Fig. 2. The aim is to show how the proposed distributed finite-time control (12), despite the presence of communication time-varying delays, can ensure a desired voltage restoration by eliminating unavoidable deviations due to primary droop-control. The system operates in islanded mode and consist of $N = 5$ droop control DG units setting on buses 1, 2, 3, 6 and 8, $M = 9$ ZIP-modeled local loads and twenty transmission lines (see the electrical power line topology in 2). Information about lines impedance and active and reactive power limits are provided according to [58], while the parameter of both droop-controlled DG

TABLE 1. DGs Locations, static droop coefficient and time constants of the LCL filters.

		DG1	DG2	DG3	DG4	DG5
DGs	Location	1	2	3	6	8
	τ_{P_i}	0.016	0.016	0.016	0.016	0.016
	τ_{Q_i}	0.016	0.016	0.016	0.016	0.016
	k_{P_i}	$3.01e^{-5}$	$7.14e^{-5}$	$1e^{-5}$	$1e^{-5}$	$1e^{-5}$
	k_{Q_i}	0.01	0.02	$2.5e^{-3}$	$4.17e^{-3}$	$4.17e^{-3}$
	k_{v_i}	$1e^{-2}$	$1e^{-2}$	$1e^{-2}$	$1e^{-2}$	$1e^{-2}$

TABLE 2. ZIP load model parameters.

Load Bus	$P_{1\rho}$	$P_{2\rho}$	$P_{3\rho}$	$Q_{1\rho}$	$Q_{2\rho}$	$Q_{3\rho}$
4	0.01	1	e^4	0.01	1	e^4
5	0.01	2	e^4	0.01	2	e^4
7	0.01	3	e^4	0.01	3	e^4
9	0.01	4	e^4	0.01	4	e^4
10	0.01	1	e^4	0.01	1	e^4
11	0.01	2	e^4	0.01	2	e^4
12	0.01	3	e^4	0.01	3	e^4
13	0.01	4	e^4	0.01	4	e^4
14	0.01	1	e^4	0.01	1	e^4

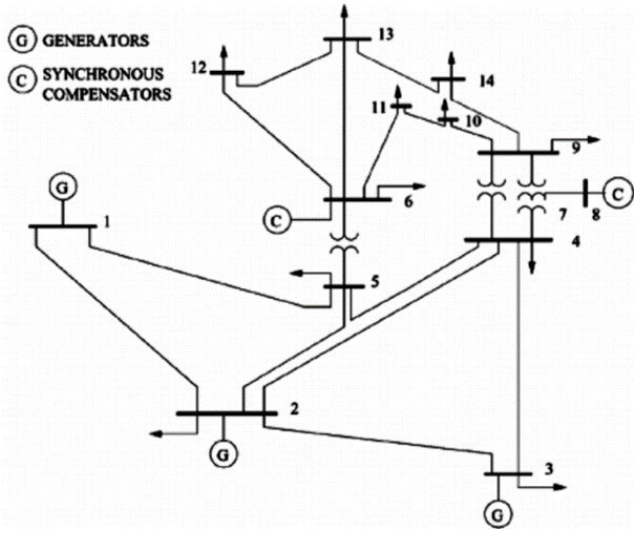

FIGURE 2. The IEEE 14-bus Test System.

units and ZIP local loads are chosen as in Table 1 and 2, respectively.

The DGs share information via the communication network topology $\mathcal{G}^c_{N+1}$ with $\mathcal{E}^c_{N+1} = \{(0, 1), (1, 2), (2, 3), (3, 2), (3, 4), (4, 5)\}$, where only DG1 has a direct access to virtual leader information. We remark that this connected communication topology is just one among all the possible configuration that can be dealt with the proposed approach (similar results have been omitted here for the sake of brevity).

In the simulation scenario, the communication delay $\tau(t)$ has been simulated as a time-varying function with a maximum value of $\tau^\star = 0.1[s]$. Note that, by considering $\tau^\star = 0.1[s]$, we have an upper bound for the communication delays that is greater than the typical maximum value allowed for wireless channel in normal operating conditions (which is about $10^{-2}[s]$ [11]). In so doing, we provide a meaningful margin of robust stability w.r.t. hard delays which correspond to sudden information packet losses. [27].

The control gains for the frequency control law in (7) are selected as $\alpha_i = 10.5$, $\beta_i = -0.3$, and $\gamma = 0.001$ [7].

Voltage regulation performances are evaluated leveraging the Matlab/Simulink simulation platform, while the LMIs defined in Theorem 1 are numerically verified by using the interior-point method implemented in Yalmip Toolbox through the SeDuMi solver. The resulting control gains in (12), obtained by verifying the feasibility problem of LMIs (15)-(16) through Yalmip Toolbox via SeDuMi solver, are $K = [-0.930 \quad -0.726]$; instead, the weighted $\mathcal{L}_2$ gain and the threshold for state trajectories are $\gamma = 0.94237$ and $c_2 = 0.0459$, respectively.

Note that, as already stated, for solving the LMIs, we have considered a fixed value for $\tau^\star$ according to technological constraints [11]. However, this parameter plays an important role for the stability of the whole MG as well as for solving the LMI problem (15)-(16). Therefore, before describing the simulation results, we have carried out a sensitivity analysis of this parameter with respect to L_2 gain γ and state trajectories threshold c_2 in order to disclose the maximum upper bound of communication delays which guarantees that Theorem 1 still holds as well as the feasibility of LMI problem is confirmed. Specifically, this latter has been verified for different value of $\tau^\star$, raging from $0.1[s]$ to $0.9[s]$ with an iterative step of $0.1[s]$. By solving the LMIs problem for each of the selected value for $\tau^\star$, we obtain different values for the $\mathcal{L}_2$ gain γ and state trajectories bound c_2 as shown in Fig. 3. This sensitivity analysis allows finding a stability margin w.r.t. the upper bound of the communication delay that can be useful if hard delays occur.

In order to disclose the strength and the robustness of the suggested finite-time control law in ensuring the achievement of voltage restoration to the set point despite the presence of both communication delays and frequency/voltage deviations, we consider a time-interval of $60[s]$ for simulation purpose. Specifically, we consider three representative simulation scenarios, namely: *i*) *nominal scenario*, where only voltages reference variations occur; *ii*) *loads changing scenario*, where both voltages reference and loads variations occur; *iii*) *plug-and-play scenario*, where we consider the more troublesome simulation scenario where plug-and-play phenomena and load variations occur. Furthermore, the validation on the IEEE 30 bus test system is carried out to disclose the applicability of the proposed approach to larger power network, while a comparison analysis is also provide to show the benefit of the approach w.r.t. the very recent technical literature.

A. NOMINAL SCENARIO

In this nominal scenario, no loads variations are considered. Particularly, the use-case under test performs only voltage reference changes, i.e.: *i*) at $t = 0$ $[s]$ the frequency and

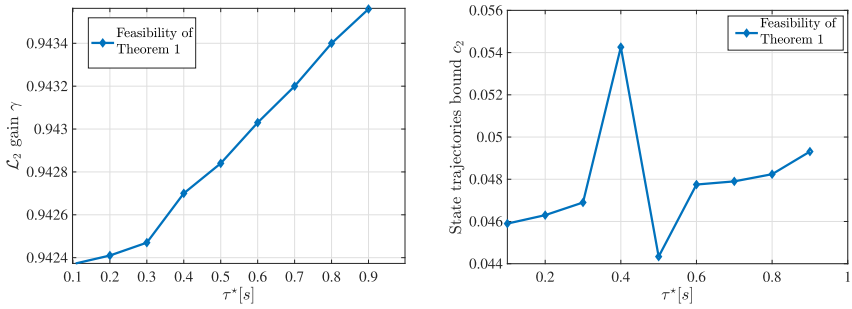

FIGURE 3. Feasibility of LMI (15) and (16) for different value of $\tau^\star \in [0.1; 0.9][s]$: a) Relation among $\tau^\star$ and L_2 gain γ; b) Relation among $\tau^\star$ and c_2.

voltage control are enabled with $\omega_0(t) = 1$ $[p.u.]$ and $v_0(t) = 1.02$ $[p.u.]$; *ii*) at $t = 10$ $[s]$ the set-point for the voltage secondary controller is set to $v_0(t) = 1.03$ $[p.u.]$; *iii*) at $t = 40$ $[s]$ the set-point restores to $v_0(t) = 1.02$ $[p.u.]$.

The effectiveness of the proposed finite-time control strategy is confirmed by the results in Fig. 4, where it is possible to appreciate the voltage synchronization process in spite of the effects of time-varying latency, the unavoidable fluctuation due to PC and the reference changes. Specifically, by activating our controller at $t = 0$ $[s]$, all the DGs voltages achieve the set-point in $T^f = 6$ $[s]$ as shown in Fig. 4(a), thus allowing the voltage errors fast approaching to zero value (see Fig. 4(b)). For completeness, Fig. 4(c) reports the frequency evolution of all the DGs under the action of (7). Finally, state trajectories evolution are disclosed in Fig. 4(d), thus confirming the boundedness of the whole Microgrid with respect to the threshold c_2, properly computed by solving LMI (16), i.e. $\tilde{x}^\top(t)\Psi\tilde{x}(t) < c_2 \quad \forall t \in [t_0, t_0 + T^f]$, being t_0 the time instant when the set-points change.

B. LOAD CHANGING SCENARIO

Since load demand is subjected to frequent changes according to specific and practical requirement, the evaluation of the robustness w.r.t. load variations is a crucial aspect to be investigated for assessing the performance of the controlled grid, besides the previous one. In particular, we consider a variable load profile $L(t)$ as depicted in Fig. 5, where a maximum load variation of $\pm$ 50% can be observed. Specifically, the following scenario is taken into account:

- At $t = 0$ $[s]$, the frequency and voltage controller are switched on, with $\omega_0 = 1$ $[p.u.]$ and $v_0 = 1.02$ $[p.u.]$;
- At $t = 10$ $[s]$, the set-point for voltage control varies to $v_0(t) = 1.03$ $[p.u.]$;
- At $t = 20$ $[s]$, there is a 30% of increasing for the nominal values of the loads;
- At $t = 30$ $[s]$, loads increase of an additional 20%;
- At $t = 40$ $[s]$ the voltages reference value is restored to $v_0(t) = 1.02$ $[p.u.]$;
- At $t = 50$ $[s]$, loads are restored to their nominal value.

Results in Fig. 6 show that the proposed approach is able to counteract the sudden variation in the load request, recovering the desired voltage intensity. Moreover, the robustness and the effectiveness of the suggested finite-time distributed controller are confirmed in Fig. 6 even in this troubled scenario characterized of sudden load changes. Specifically, as the SC is switched on at $t = 0$ $[s]$, the voltages of all DG units restore to the set-point in $T^f = 6$ $[s]$ as shown Fig. 6(a) and the voltage errors w.r.t. the references go to zero (see Fig. 6(b)). Load variation and voltage references changes are performed at the next step of the simulation and the same good performance are achieved in this scenario as well. Indeed, also in this case, the proposed controller allows adjusting the voltages of all the DGs to the desired reference value with the same settling time $T^f = 6$ $[s]$. Obviously, tolerable errors can be seen in the voltage time evolution in Fig. 6(a)-(b) in concurrence of load fluctuations. Fig. 6(c) points out the time evolution of the DGs frequency with controller in (7) switched on. Furthermore, according to Definition 1, Fig. 6(d) proves the boundedness of the overall state trajectories, i.e. $\tilde{x}^\top(t)\Psi\tilde{x}(t) < c_2 \quad \forall t \in [t_0, t_0 + T^f]$, where t_0 is the time instant when sudden changes in loads and references appear.

C. PLUG-AND-PLAY SCENARIO

Here we discuss the robustness of the proposed control approach in the more troublesome simulation scenario where plug-and-play phenomena and load variations, as in in Fig. 5, occur. More specifically, we consider that DG2 at bus 2 and DG4 at bus 6 are unplugged at $t = 25[s]$ and $t = 50[s]$ respectively, and then plugged-in at $t = 32[s]$ and $t = 52[s]$ respectively. Note that these sources failure also implies communication losses for the links connected to the unplugged DGS [59]. Simulation results, depicted in Fig. 7, confirm the effectiveness of the proposed

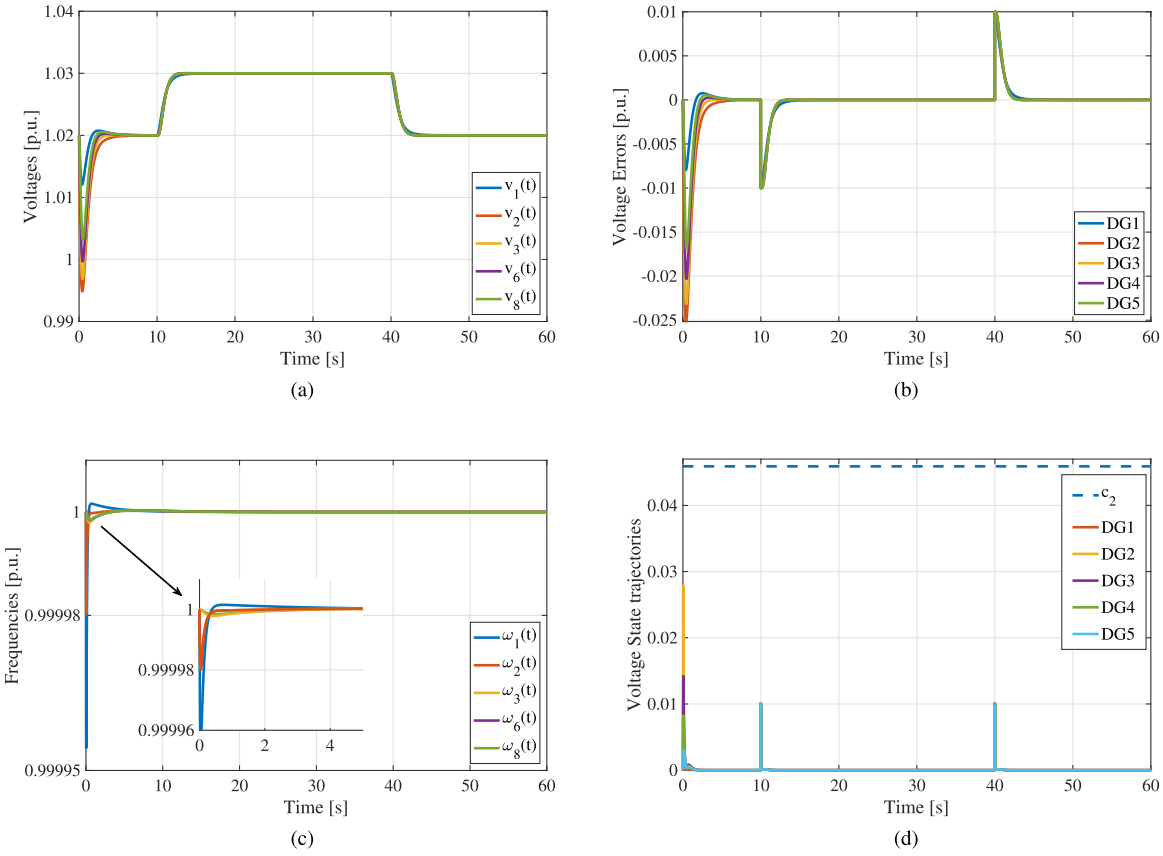

FIGURE 4. Distributed Finite-Time Voltage Restoration Control in the *nominal scenario*. Time history of: a) voltage $v_i(t), i = 1, \ldots, 5$; b) voltage error $v_i(t) - v_0(t), i = 1, \ldots, 5$; c) frequency $\omega_i(t), i = 1, \ldots, 5$; d) Voltage state trajectories $\tilde{x}^\top(t)\Psi\tilde{x}(t)$.

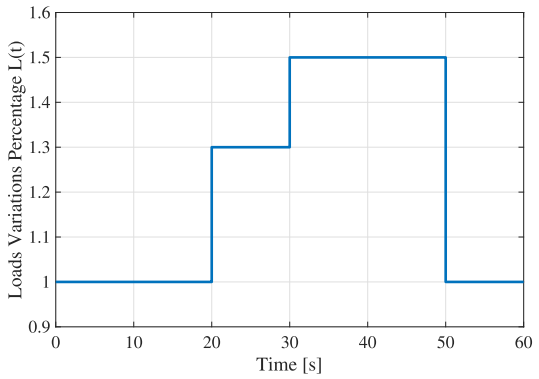

FIGURE 5. Distributed Finite-Time Voltage Restoration Control in the *load changing scenario*. Time history of the loads percentage variation with respect to the nominal values.

control approach in ensuring finite-time voltage control also in this troublesome electrical scenario. Specifically, Fig. 7(a) shows that voltage controllers successfully face to DGs losses by sharing the excess power among the remaining DG units (see Fig 7(b)). Finally as highlighted in Fig. 7(c), the boundedness of the overall state-trajectories is still guaranteed.

D. VALIDATION ON A LARGER SYSTEM: THE CASE OF IEEE 30 BUS TEST SYSTEM

In section we aim at corroborating the applicability of the proposed control approach also in larger system with more interconnected DG units sharing information via a communication network affected by time-varying communication delays. More specifically, we consider the IEEE 30-bus system operating in stand-alone mode and consisting of $N = 7$ droop control DG units, set on buses 1, 2, 3, 6, 8, 10 and 13, $M = 23$ ZIP local loads and 41 transmission lines, whose parameters are given in [58]. As exemplar simulation scenario we consider the *nominal scenario* as described in Section VI.A. Results in Fig. 8 disclose that, also for larger power networks, the proposed control protocol (12) is able to ensure the robust finite-time voltage regulation problem despite the presence of communication time-varying delays. Indeed, all the DG units track the reference behaviour (see Fig. 8(a)-(b)) while counteracting the effects of communication latency as well as the natural deviation due to underlying control layer. Finally, the boundedness of the state trajectories evolution is still guaranteed as shown in Fig. 8(c), thus confirming that $\tilde{x}^\top\Psi\tilde{x} < c_2 \forall t \in [t_0, t_0 + T^f]$, being t_0 the time instant when reference variations occur. The obtained results confirm how our approach successes in guaranteeing the control

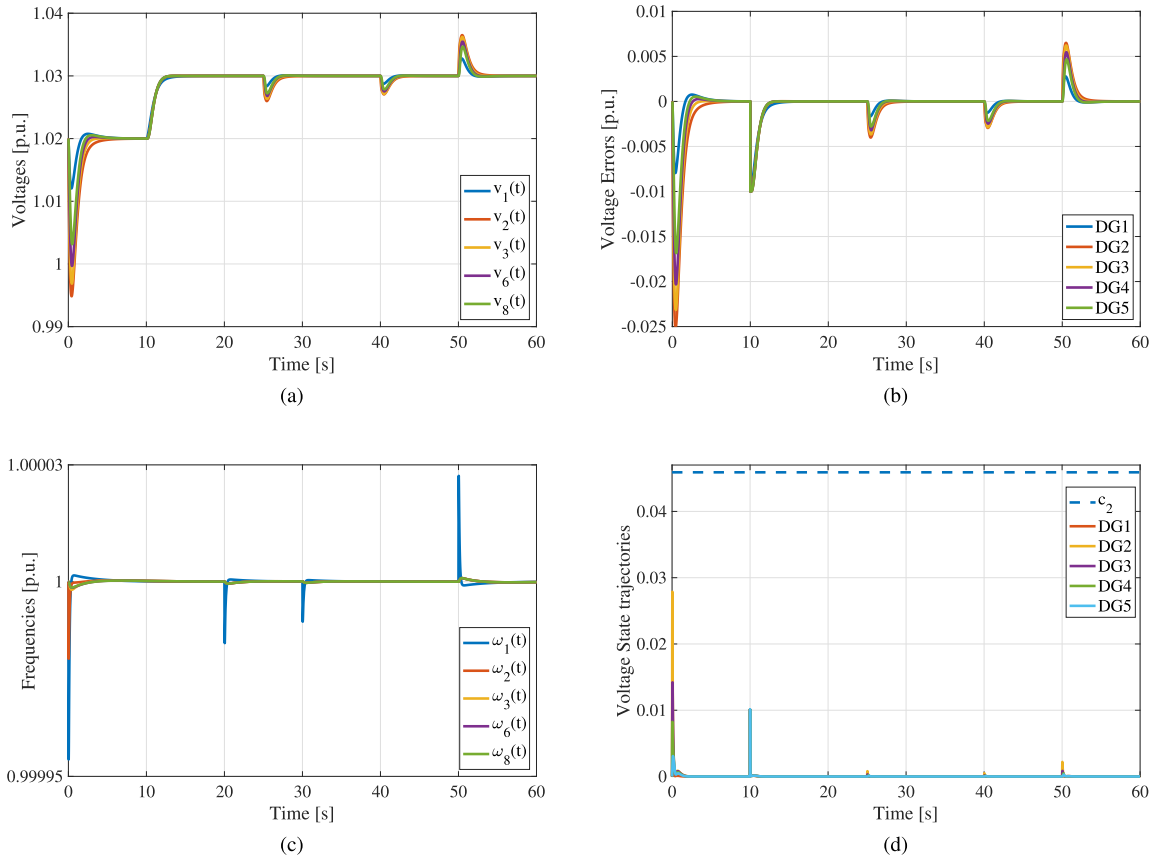

FIGURE 6. Distributed Finite-Time Voltage Restoration Control in the *load changing scenario*. Time history of: a) voltage $v_i(t), i = 1, \ldots, 5$; b) voltage error $v_i(t) - v_0(t), i = 1, \ldots, 5$; c) frequency $\omega_i(t), i = 1, \ldots, 5$; d) Voltage state trajectories $\tilde{x}^\top(t)\Psi\tilde{x}(t)$.

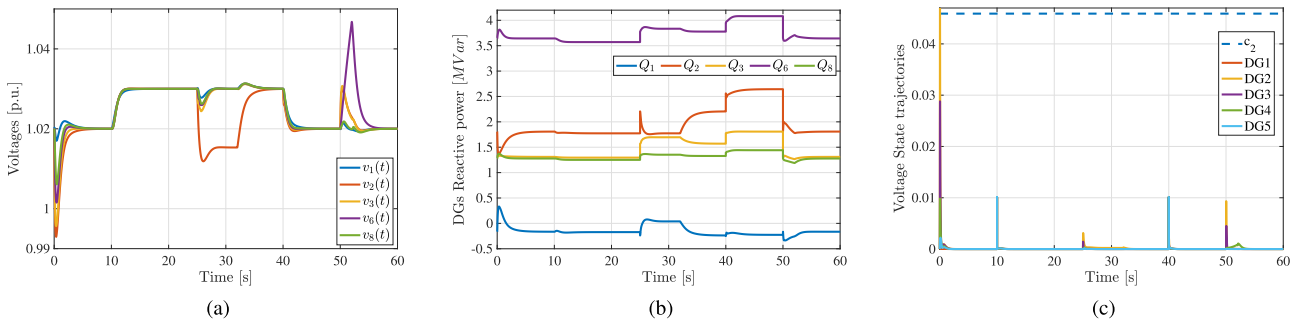

FIGURE 7. Plug-and-Play scenario for DG2 and DG4 in *load changing scenario*. Time history of: a) voltage $v_i(t), i = 1, \ldots, 5$; b) supplied reactive power $Q_i(t), i = 1, \ldots, 5$; c) Voltage state trajectories $\tilde{x}^\top(t)\Psi\tilde{x}(t)$.

objectives, as stated in Section IV, for larger test-bus power network.

E. COMPARISON ANALYSIS

To further disclose the benefit of our finite-time networked-based delayed control input in guaranteeing voltage regulation in MG, herein we compare the obtained performances with the ones achievable via the nonlinear distributed voltage controller, very recently proposed in [18], which neglects the unavoidable presence of communication impairments. For the comparison analysis, we consider the *nominal scenario* as detailed in Section VI-A. The performances achievable with the nonlinear controller [18] are disclosed in Fig. 9 which highlights how time-varying delays dramatically affect the Microgrids stability. By observing both Fig. 4 and Fig. 9, we can appreciate how the proposed control approach allows achieving improved performances in terms voltage regulation while counteracting time-varying communication delays as well as voltage deviations due to primary control layer and references variations. We remark

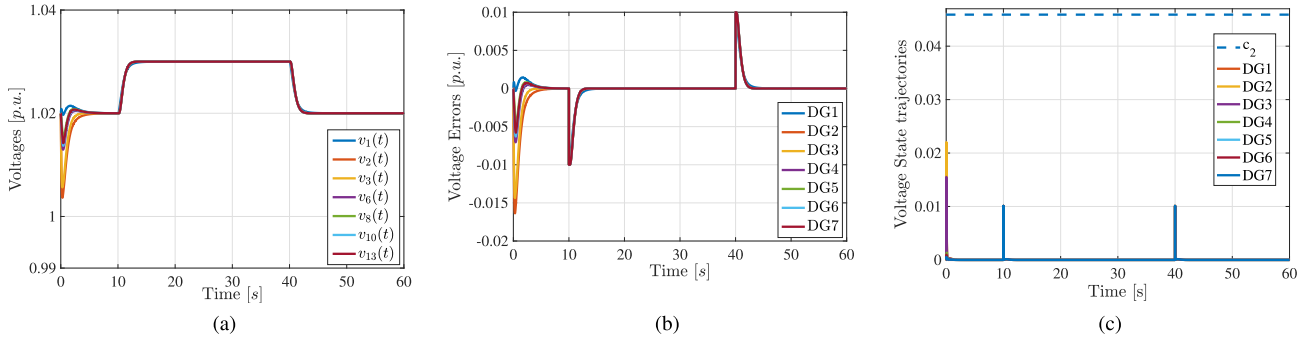

FIGURE 8. Distributed Finite-Time Voltage Restoration Control in the *nominal scenario* for IEEE 30 bus Test System. Time history of: a) voltage $v_i(t), i = 1, \ldots, 7$; b) voltage errors $v_i(t) - v_0(t), i = 1, \ldots, 7$; c) Voltage state trajectories $\tilde{x}^\top(t)\Psi\tilde{x}(t)$.

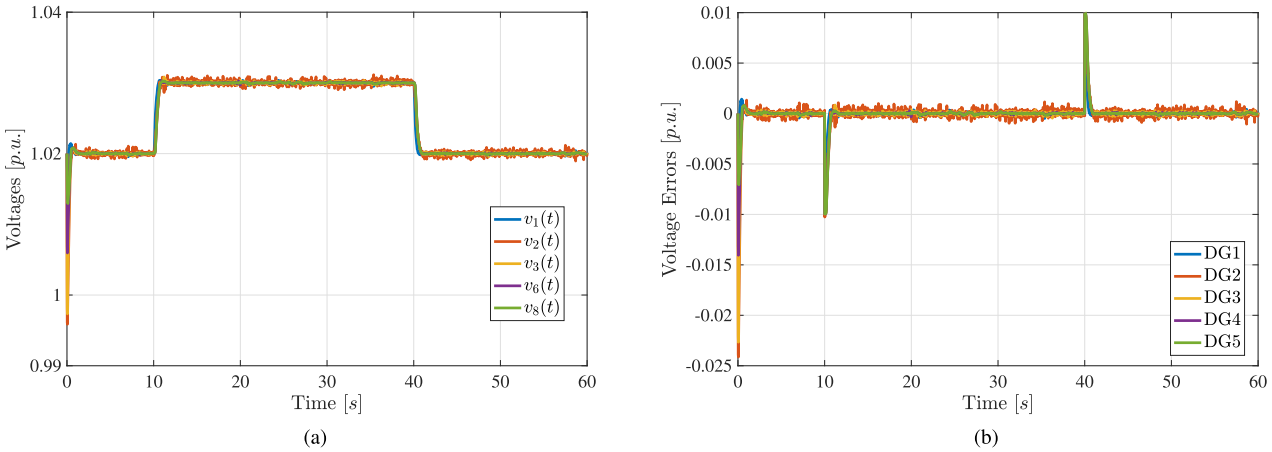

FIGURE 9. Comparison with nonlinear controller proposed in [18] for the *nominal scenario*. Time history of: a) voltage $v_i(t), i = 1, \ldots, 5$; b) voltage errors $v_i(t) - v_0(t), i = 1, \ldots, 5$.

that this benefit is due to the fact that the communication delays are taken into account from the beginning of the control design phase.

VII. CONCLUSION

In this paper, the problem of secondary voltage restoration in stand-alone inverter-based Microgrid has been investigated and solved via a fully distributed finite-time control protocol. Exploiting Lypunov-Krasosovskii theory combined with Finite-Time Stability tools, we have analytically demonstrated the effectiveness and the robustness of the proposed control law in ensuring that each DG unit within the Microgrid tracks the leader behaviour despite the presence of time-varying communication delays. The derived delay-dependent stability criteria, expressed as a set of LMIs, allows tuning the robust control gains vector. An extensive numerical simulation, carried out on a realistic case study using the popular benchmark of the IEEE 14 bus test system, has been performed. Numerical results have revealed the robustness and the effectiveness of the proposed control architecture in guaranteeing that all the DGs involved in the MG track the reference leader behaviour with specified transient and steady-state performances, in spite of the presence of communication time-varying latencies, as well as natural voltage fluctuations induced by the primary control layer.

Future work could include: *i*) the extension of the proposed networked-based approach to solve resilience problem w.r.t. communication links losses and agent faults; *ii*) the practical implementation of the proposed control scheme in real time MG.

REFERENCES

[1] A. Cagnano, A. C. Bugliari, and E. De Tuglie, "A cooperative control for the reserve management of isolated microgrids," *Appl. Energy*, vol. 218, pp. 256–265, May 2018.

[2] A. M. Bouzid, J. M. Guerrero, A. Cheriti, M. Bouhamida, P. Sicard, and M. Benghanem, "A survey on control of electric power distributed generation systems for microgrid applications," *Renew. Sustain. Energy Rev.*, vol. 44, pp. 751–766, Apr. 2015.

[3] L. Mariam, M. Basu, and M. F. Conlon, "Microgrid: Architecture, policy and future trends," *Renew. Sustain. Energy Rev.*, vol. 64, pp. 477–489, Oct. 2016.

[4] J. J. Justo, F. Mwasilu, J. Lee, and J.-W. Jung, "AC-microgrids versus DC-microgrids with distributed energy resources: A review," *Renew. Sustain. Energy Rev.*, vol. 24, pp. 387–405, Aug. 2013.

[5] S. Kakran and S. Chanana, "Smart operations of smart grids integrated with distributed generation: A review," *Renew. Sustain. Energy Rev.*, vol. 81, pp. 524–535, Jan. 2018.

[6] M. H. Andishgar, E. Gholipour, and R.-A. Hooshmand, "An overview of control approaches of inverter-based microgrids in islanding mode of operation," *Renew. Sustain. Energy Rev.*, vol. 80, pp. 1043–1060, Dec. 2017.
[7] F. Guo, C. Wen, J. Mao, and Y.-D. Song, "Distributed secondary voltage and frequency restoration control of droop-controlled inverter-based microgrids," *IEEE Trans. Ind. Electron.*, vol. 62, no. 7, pp. 4355–4364, Jul. 2015.
[8] M. F. Roslan, M. A. Hannan, P. J. Ker, and M. N. Uddin, "Microgrid control methods toward achieving sustainable energy management," *Appl. Energy*, vol. 240, pp. 583–607, Apr. 2019.
[9] M. A. Shahab, B. Mozafari, S. Soleymani, N. M. Dehkordi, H. M. Shourkaei, and J. M. Guerrero, "Distributed consensus-based fault tolerant control of islanded microgrids," *IEEE Trans. Smart Grid*, vol. 11, no. 1, pp. 37–47, Jan. 2020.
[10] W. F. Tinney and C. E. Hart, "Power flow solution by Newton's method," *IEEE Trans. Power App. Syst.*, vol. PAS-86, no. 11, pp. 1449–1460, Nov. 1967.
[11] A. Andreotti, B. Caiazzo, A. Petrillo, S. Santini, and A. Vaccaro, "Decentralized smart grid voltage control by synchronization of linear multiagent systems in the presence of time-varying latencies," *Electronics*, vol. 8, no. 12, p. 1470, Dec. 2019.
[12] Q. Shafiee, J. M. Guerrero, and J. C. Vasquez, "Distributed secondary control for islanded microgrids—A novel approach," *IEEE Trans. Power Electron.*, vol. 29, no. 2, pp. 1018–1031, Feb. 2014.
[13] Y. Han, K. Zhang, H. Li, E. A. A. Coelho, and J. M. Guerrero, "MAS-based distributed coordinated control and optimization in microgrid and microgrid clusters: A comprehensive overview," *IEEE Trans. Power Electron.*, vol. 33, no. 8, pp. 6488–6508, Aug. 2018.
[14] A. Andreotti, A. Petrillo, S. Santini, A. Vaccaro, and D. Villacci, "A decentralized architecture based on cooperative dynamic agents for online voltage regulation in smart grids," *Energies*, vol. 12, no. 7, p. 1386, 2019.
[15] Y. Wang, T. L. Nguyen, Y. Xu, Z. Li, Q.-T. Tran, and R. Caire, "Cyber-physical design and implementation of distributed event-triggered secondary control in islanded microgrids," *IEEE Trans. Ind. Appl.*, vol. 55, no. 6, pp. 5631–5642, Nov. 2019.
[16] Z. Li, Z. Cheng, J. Liang, J. Si, L. Dong, and S. Li, "Distributed event-triggered secondary control for economic dispatch and frequency restoration control of droop-controlled AC microgrids," *IEEE Trans. Sustain. Energy*, vol. 11, no. 3, pp. 1938–1950, Jul. 2020.
[17] N. M. Dehkordi, H. R. Baghaee, N. Sadati, and J. M. Guerrero, "Distributed noise-resilient secondary voltage and frequency control for islanded microgrids," *IEEE Trans. Smart Grid*, vol. 10, no. 4, pp. 3780–3790, Jul. 2019.
[18] J. Liu, J. Li, H. Song, A. Nawaz, and Y. Qu, "Nonlinear secondary voltage control of islanded microgrid via distributed consistency," *IEEE Trans. Energy Convers.*, vol. 35, no. 4, pp. 1964–1972, Dec. 2020.
[19] Z. Cheng, Z. Li, J. Liang, J. Gao, J. Si, and S. Li, "Distributed economic power dispatch and bus voltage control for droop-controlled DC microgrids," *Energies*, vol. 12, no. 7, p. 1400, Apr. 2019.
[20] X. Wu, L. Chen, C. Shen, Y. Xu, J. He, and C. Fang, "Distributed optimal operation of hierarchically controlled microgrids," *IET Gener., Transmiss. Distrib.*, vol. 12, no. 18, pp. 4142–4152, Oct. 2018.
[21] J. Lai and X. Lu, "Nonlinear mean-square power sharing control for AC microgrids under distributed event detection," *IEEE Trans. Ind. Informat.*, vol. 17, no. 1, pp. 219–229, Jan. 2021.
[22] J. Lai, X. Lu, X. Yu, and A. Monti, "Stochastic distributed secondary control for AC microgrids via event-triggered communication," *IEEE Trans. Smart Grid*, vol. 11, no. 4, pp. 2746–2759, Jul. 2020.
[23] X. Lu, X. Yu, J. Lai, J. M. Guerrero, and H. Zhou, "Distributed secondary voltage and frequency control for islanded microgrids with uncertain communication links," *IEEE Trans. Ind. Informat.*, vol. 13, no. 2, pp. 448–460, Apr. 2017.
[24] Y. Han, H. Li, P. Shen, E. A. A. Coelho, and J. M. Guerrero, "Review of active and reactive power sharing strategies in hierarchical controlled microgrids," *IEEE Trans. Power Electron.*, vol. 32, no. 3, pp. 2427–2451, Mar. 2017.
[25] G. Lou, W. Gu, J. Wang, W. Sheng, and L. Sun, "Optimal design for distributed secondary voltage control in islanded microgrids: Communication topology and controller," *IEEE Trans. Power Syst.*, vol. 34, no. 2, pp. 968–981, Mar. 2019.
[26] J. Lai, X. Lu, X. Yu, A. Monti, and H. Zhou, "Distributed voltage regulation for cyber-physical microgrids with coupling delays and slow switching topologies," *IEEE Trans. Syst., Man, Cybern. Syst.*, vol. 50, no. 1, pp. 100–110, Jan. 2020.
[27] A. Petrillo, A. Pescape, and S. Santini, "A secure adaptive control for cooperative driving of autonomous connected vehicles in the presence of heterogeneous communication delays and cyberattacks," *IEEE Trans. Cybern.*, vol. 51, no. 3, pp. 1134–1149, Mar. 2021.
[28] J. Lai, H. Zhou, X. Lu, X. Yu, and W. Hu, "Droop-based distributed cooperative control for microgrids with time-varying delays," *IEEE Trans. Smart Grid*, vol. 7, no. 4, pp. 1775–1789, Jul. 2016.
[29] P. Tong, S. Chen, and L. Wang, "Finite-time consensus of multi-agent systems with continuous time-varying interaction topology," *Neurocomputing*, vol. 284, pp. 187–193, Apr. 2018.
[30] N. M. Dehkordi, N. Sadati, and M. Hamzeh, "Distributed robust finite-time secondary voltage and frequency control of islanded microgrids," *IEEE Trans. Power Syst.*, vol. 32, no. 5, pp. 3648–3659, Sep. 2017.
[31] Y. Xu and H. Sun, "Distributed finite-time convergence control of an islanded low-voltage AC microgrid," *IEEE Trans. Power Syst.*, vol. 33, no. 3, pp. 2339–2348, May 2018.
[32] A. Pilloni, A. Pisano, and E. Usai, "Robust finite-time frequency and voltage restoration of inverter-based microgrids via sliding-mode cooperative control," *IEEE Trans. Ind. Electron.*, vol. 65, no. 1, pp. 907–917, Jan. 2018.
[33] B. Ning, Q.-L. Han, and L. Ding, "Distributed finite-time secondary frequency and voltage control for islanded microgrids with communication delays and switching topologies," *IEEE Trans. Cybern.*, early access, Sep. 16, 2020, doi: 10.1109/TCYB.2020.3003690.
[34] A. Andreotti, B. Caiazzo, A. Petrillo, S. Santini, and A. Vaccaro, "Robust finite-time voltage restoration in inverter-based microgrids via distributed cooperative control in presence of communication time-varying delays," in *Proc. IEEE Int. Conf. Environ. Electr. Eng., IEEE Ind. Commercial Power Syst. Eur. (EEEIC/I&CPS Europe)*, Jun. 2020, pp. 1–6.
[35] J. Lai, X. Lu, and A. Monti, "Distributed secondary voltage control for autonomous microgrids under additive measurement noises and time delays," *IET Gener., Transmiss. Distrib.*, vol. 13, no. 14, pp. 2976–2985, Jul. 2019.
[36] F. L. Lewis, H. Zhang, K. Hengster-Movric, and A. Das, *Cooperative Control of Multi-Agent Systems: Optimal and Adaptive Design Approaches*. Berlin, Germany: Springer, 2013.
[37] E. Fridman, *Introduction to Time-Delay Systems: Analysis and Control*. Berlin, Germany: Springer, 2014.
[38] X. Yang, X. Li, and J. Cao, "Robust finite-time stability of singular nonlinear systems with interval time-varying delay," *J. Franklin Inst.*, vol. 355, no. 3, pp. 1241–1258, Feb. 2018.
[39] S. He, J. Song, and F. Liu, "Robust finite-time bounded controller design of time-delay conic nonlinear systems using sliding mode control strategy," *IEEE Trans. Syst., Man, Cybern. Syst.*, vol. 48, no. 11, pp. 1863–1873, Nov. 2018.
[40] J. Schiffer, D. Zonetti, R. Ortega, A. M. Stanković, T. Sezi, and J. Raisch, "A survey on modeling of microgrids—From fundamental physics to phasors and voltage sources," *Automatica*, vol. 74, pp. 135–150, Dec. 2016.
[41] Y. Peng, Z. Shuai, X. Liu, Z. Li, J. M. Guerrero, and Z. J. Shen, "Modeling and stability analysis of inverter-based microgrid under harmonic conditions," *IEEE Trans. Smart Grid*, vol. 11, no. 2, pp. 1330–1342, Mar. 2020.
[42] Y. Wu, Y. Wu, J. M. Guerrero, J. C. Vasquez, and J. Li, "AC microgrid small-signal modeling: Hierarchical control structure challenges and solutions," *IEEE Electrific. Mag.*, vol. 7, no. 4, pp. 81–88, Dec. 2019.
[43] K. Mahmud, A. K. Sahoo, J. Ravishankar, and Z. Y. Dong, "Coordinated multilayer control for energy management of grid-connected AC microgrids," *IEEE Trans. Ind. Appl.*, vol. 55, no. 6, pp. 7071–7081, Nov. 2019.
[44] S. Shrivastava, B. Subudhi, and S. Das, "Distributed voltage and frequency synchronisation control scheme for islanded inverter-based microgrid," *IET Smart Grid*, vol. 1, no. 2, pp. 48–56, Jul. 2018.
[45] K. De Brabandere, B. Bolsens, J. Van den Keybus, A. Woyte, J. Driesen, and R. Belmans, "A voltage and frequency droop control method for parallel inverters," *IEEE Trans. Power Electron.*, vol. 22, no. 4, pp. 1107–1115, Jul. 2007.
[46] J. Schiffer, R. Ortega, A. Astolfi, J. Raisch, and T. Sezi, "Conditions for stability of droop-controlled inverter-based microgrids," *Automatica*, vol. 50, no. 10, pp. 2457–2469, Oct. 2014.
[47] J. M. Guerrero, M. Chandorkar, T.-L. Lee, and P. C. Loh, "Advanced control architectures for intelligent microgrids—Part I: Decentralized and hierarchical control," *IEEE Trans. Ind. Electron.*, vol. 60, no. 4, pp. 1254–1262, Apr. 2012.
[48] J. Schiffer, T. Seel, J. Raisch, and T. Sezi, "Voltage stability and reactive power sharing in inverter-based microgrids with consensus-based distributed voltage control," *IEEE Trans. Control Syst. Technol.*, vol. 24, no. 1, pp. 96–109, Jan. 2016.

[49] J. J. Grainger, W. D. Stevenson, and W. D. Stevenson, *Power System Analysis* (McGraw-Hill Series in Electrical and Computer Engineering. Power and Energy). New York, NY, USA: McGraw-Hill, 2003.
[50] M. S. Hossan, H. M. Maruf, and B. Chowdhury, "Comparison of the zip load model and the exponential load model for CVR factor evaluation," in *Proc. IEEE Power Energy Soc. Gen. Meeting*, Jul. 2017, pp. 1–5.
[51] A. Petrillo, A. Salvi, S. Santini, and A. S. Valente, "Adaptive synchronization of linear multi-agent systems with time-varying multiple delays," *J. Franklin Inst.*, vol. 354, no. 18, pp. 8586–8605, Dec. 2017.
[52] M. Gholami, A. Pilloni, A. Pisano, Z. A. S. Dashti, and E. Usai, "Robust consensus-based secondary voltage restoration of inverter-based islanded microgrids with delayed communications," in *Proc. IEEE Conf. Decis. Control (CDC)*, Dec. 2018, pp. 811–816.
[53] S. Sahoo and S. Mishra, "A distributed finite-time secondary average voltage regulation and current sharing controller for DC microgrids," *IEEE Trans. Smart Grid*, vol. 10, no. 1, pp. 282–292, Jan. 2019.
[54] G. Fiengo, D. G. Lui, A. Petrillo, and S. Santini, "Distributed leader-tracking adaptive control for high-order nonlinear lipschitz multi-agent systems with multiple time-varying communication delays," *Int. J. Control*, pp. 1–13, Nov. 2019, doi: 10.1080/00207179.2019.1683608.
[55] S. Boyd, L. El Ghaoui, E. Feron, and V. Balakrishnan, *Linear Matrix Inequalities in System and Control Theory*, vol. 15. Philadelphia, PA, USA: SIAM, 1994.
[56] J. Lofberg, "YALMIP: A toolbox for modeling and optimization in MATLAB," in *Proc. IEEE Int. Conf. Robot. Automat.*, Sep. 2004, pp. 284–289.
[57] Z. Xiang, Y.-N. Sun, and M. S. Mahmoud, "Robust finite-time H_∞ control for a class of uncertain switched neutral systems," *Commun. Nonlinear Sci. Numer. Simul.*, vol. 17, no. 4, pp. 1766–1778, 2012.
[58] R. D. Zimmerman and C. E. Murillo-Sánchez, "Matpower 6.0 user's manual," *Power Syst. Eng. Res. Center*, vol. 9, 2016. [Online]. Available: https://matpower.org/docs/MIPS-manual-1.4.pdf
[59] V. Nasirian, Q. Shafiee, J. M. Guerrero, F. L. Lewis, and A. Davoudi, "Droop-free distributed control for AC microgrids," *IEEE Trans. Power Electron.*, vol. 31, no. 2, pp. 1600–1617, Feb. 2016.

AMEDEO ANDREOTTI (Senior Member, IEEE) received the M.S. and Ph.D. degrees in electrical engineering from the University of Naples Federico II. He is currently an Associate Professor with the University of Naples Federico II. He is the author or coauthor of more than 200 scientific publications in reviewed journals and international conferences. His research interests include transients in power systems, lightning effects on power systems, electromagnetic compatibility, power quality, and smart grids. He is also an Editor of IEEE TRANSACTIONS ON POWER DELIVERY and an Associate Editor of IEEE ACCESS, *High Voltage* (IET), and *Electrical Engineering* (Springer). He is a member of the IEEE Working Group Lightning Performance of Distribution Lines and has been a member of the section MT600 of the TC1 of the International Electrotechnical Commission.

BIANCA CAIAZZO received the M.Sc. degree in management engineering from the University of Naples Federico II. She was submitting the thesis Distributed Cooperative Finite-Time control for multi-platoon of autonomous connected vehicles in the presence of communication impairments. She is currently pursuing the Ph.D. degree in information technology and electrical engineering, Cycle: XXXV. Her research interest includes dynamics and control of power networks.

ALBERTO PETRILLO received the Ph.D. degree in control systems engineering from the University of Naples Federico II, in 2019. He is currently a Research Fellow with the University of Naples Federico II. His work mainly focuses on the distributed, synchronization-based, control of networked control systems in the presence of communication impairments and security vulnerabilities with application to automotive field and energy systems.

STEFANIA SANTINI (Member, IEEE) received the M.Sc. degree in electronic engineering and the Ph.D. degree in automatic control from the University of Naples Federico II, Naples, Italy, in 1996 and 1999, respectively. She is currently an Associate Professor of automatic control. She is involved in many projects with industry, including small- and medium-sized enterprises operating in the automotive field. Her research interests include the area of the analysis and control of nonlinear systems with applications to automotive engineering, transportation technologies, computational biology, and energy systems.